Effect of low-energy electron interference on strong-field molecular ionization

Shilin Hu and Jing Chen*
Institute of Applied Physics and Computational Mathematics, P. O. Box 8009, Beijing 100088, China
and HEDPS, Center for Applied Physics and Technology, Collaborative Innovation Center of IFSA, Peking University, Beijing 100084, China

Xiaolei Hao and Weidong Li
Institute of Theoretical Physics and Department of Physics, Shanxi University, Taiyuan 030006, China
(Received 6 November 2015; published 24 February 2016)

By using a three-dimensional time-dependent Schrödinger equation, we calculate alignment-dependent ionization of model diatomic molecules subjected to an intense laser field with different internuclear distances. It is found that the ionization probability shows oscillatory behavior with respect to the angle between the laser polarization direction and the molecular axis for large internuclear distances. Comparing with the results obtained by Ammosov–Delone–Krainov (ADK) theory and *S*-matrix theory, the intriguing phenomenon can be attributed to the two-center interference effect of low-energy photoelectrons. Furthermore, it is shown that ADK theory is not applicable for the investigation of molecular ionization for large internuclear distances.

DOI: 10.1103/PhysRevA.93.023424

I. INTRODUCTION

Molecular ionization in strong laser fields has drawn great attention in recent years because it is a fundamental process triggering a number of important applications such as tomographic imaging of molecular orbitals and ultrafast imaging of molecular dynamics [1,2]. Compared with atoms whose ionization behavior mainly depends on their ionization energies, there are additional parameters to be taken into account for molecules, such as internuclear separations, orientation of molecular axis relative to the laser polarization direction, and interference between the partial electron wave packets ionized from different cores, which gives rise to various types of peculiar characteristics for molecular ionization [3]. For example, it is found that the ionization yield of N_2 is similar to its companion Ar atom ("companion" means that it has the analogous binding energy), while the ionization probability of the diatomic molecule O_2 is strongly suppressed with respect to the rare gas atom Xe [4–6]. Very recently, the suppressed ionization of O_2 in intense mid-infrared laser fields is unambiguously attributed to the destructive two-center interference effect [7]. Another example is the orientation dependence of ionization for CO_2 subjected to the intense laser field. In Ref. [8], the experimental data of alignment-dependent ionization for O_2 and N_2 are well reproduced by theoretical simulations, while the narrow ionization distribution of CO_2 and its peak ionization at 45° with respect to the laser field are not in agreement with the calculations [8]. Considerable efforts have been devoted to addressing this issue, but no consensus on the underlying mechanism has been achieved so far [9–12].

So far, most theoretical studies focus on the ionization dynamics of molecules with small internuclear distances [13–15]. For intermediate or large internuclear separations, charge-resonance-enhanced ionization of molecules has been studied in numerical calculations [16,17] and experiment [18]. Recently, the interference effect on the ionization dynamics of Ar_2 with large internuclear distance has been reported in experiment [19]. Afterward, interference signatures is found in electron momentum distributions of H_2^+ at large internuclear separation subjected to an intense laser field [20]. However, there has been no study on the orientation dependence of molecular ionization based on three-dimensional *ab initio* calculations for large internuclear distances (several tens of a.u.) so far. As we know, the ionization rate of diatomic homonuclear molecule with bonding valence orbital, e.g., H_2 and N_2, exposed to linear polarized laser field is relative to a factor $\cos^2(\mathbf{P}\cdot\mathbf{R}/2)$ within the framework of *S*-matrix theory [6], where $\mathbf{P}$ and $\mathbf{R}$ denote the momentum of the emitted electron and the internuclear separation, respectively. In addition, the ionization yield is dominated by the ionized electron with small momenta, so the factor $\cos^2(\mathbf{P}\cdot\mathbf{R}/2)$ plays a less important role in the ionization of molecules with small R. The impact of the factor on molecular ionization is not negligible for large R, so the effect of interference on the ionization dynamics of molecules with large internuclear separation is an intriguing problem.

II. CALCULATION AND DISCUSSION

In this paper, one-electron diatomic systems subjected to a few-cycle pulse at the near-infrared wavelength of 800 nm have been chosen to study the alignment dependence of molecular ionization because it could be accurately taken into account by solving the three-dimensional time-dependent Schrödinger equation (TDSE). For model diatomic molecules with different internuclear distances, prolate spheroidal coordinates are suitable to represent the electron. If r_1 and r_2 are the distances of the electron from two nuclei, and R is the internuclear separation, then we define $\xi = (r_1 + r_2)/R$, $\eta = (r_1 - r_2)/R$. With the fixed-nuclei approximation, the field-free Hamiltonian could be written as (atomic units are utilized in this work unless otherwise indicated)

$$H_1 = -\frac{2}{R^2(\xi^2-\eta^2)}\left[\frac{\partial}{\partial\xi}(\xi^2-1)\frac{\partial}{\partial\xi} + \frac{\partial}{\partial\eta}(1-\eta^2)\frac{\partial}{\partial\eta} + \frac{\xi^2-\eta^2}{(\xi^2-1)(1-\eta^2)}\frac{\partial^2}{\partial\varphi^2}\right] - \frac{2}{R}\left[\frac{Z_1}{\xi+\eta} + \frac{Z_1}{\xi-\eta}\right], \quad (1)$$

*chen_jing@iapcm.ac.cn

where φ is the azimuthal angle, and Z_1 is the charge of the nuclei. For internuclear distances $R = 2, 10, 20, 30$ a.u. in the following calculations, the charges of the nuclei are $Z_1 = 0.68$, 1.0, 1.047, 1.063, respectively, which ensure an energy of the $1\sigma_g$ state around -0.6 a.u. We assume that the polarization vector of the field lies in the plane x-z. Within the dipole approximation, the laser-molecule interaction term is expressed as $H_t = -\frac{R}{2}[\xi\eta\cos\beta + \sqrt{(\xi^2-1)(1-\eta^2)}\cos\varphi\sin\beta]E(t)$ in the length gauge, where β is the angle between the molecular axis and the laser polarization direction. The time-dependent electric field is defined as $\mathbf{E}(t) = -\frac{\partial \mathbf{A}(t)}{\partial t}$, and the vector potential is $\mathbf{A}(t) = \frac{E_0}{\omega}\mathbf{e}\sin^2(\pi t/t_{\max})\cos\omega t$ with unit vector $\mathbf{e}$, $0 < t < t_{\max}$. E_0 is the peak electric field, and $t_{\max}$ and ω are the duration and the frequency of the laser pulse, respectively. In this paper, the diatomic molecule is subjected to a short (3 cycles) laser pulse of frequency $\omega = 0.057$ a.u. ($\lambda = 800$ nm) and the maximum electric field $E_0 = 0.063$ a.u. corresponding to laser intensity $I = 1.4\times10^{14}$ W/cm^2. The time-dependent wave functions are expanded in terms of B splines as $\Psi(\xi,\eta,\varphi,t) = \sum_{\mu,\nu,m} C_{\mu,\nu,m}(t)(\xi^2-1)^{|m|/2}(1-\eta^2)^{|m|/2}B_\mu^k(\xi)B_\nu^k(\eta)e^{im\varphi}/\sqrt{2\pi}$, where m is magnetic quantum number, and $B_\mu^k(\xi)$ is the B-spline basis of order $k = 7$ [21,22]. The time-dependent wave functions are propagated by the Crank–Nicolson method [21,22]. At the end of the pulse, the ionization probability is calculated as $P_{\text{ion}} = 1 - \sum_n |\langle\psi_n(\mathbf{r})|\Psi(\mathbf{r},t_{\max})\rangle|^2$, where ψ_n is the bound state obtained by diagonalization of the field-free Hamiltonian matrix. The population of the electron in continuum states is defined as $\sum_\mu |\langle\psi_\mu(\mathbf{r})|\Psi(\mathbf{r},t_{\max})\rangle|^2$, where the discretized continuum state ψ_μ corresponds to the energy in a range $[n_1\omega, n_2\omega]$. In the present study, the initial state is the $1\sigma_g$ state, 160 B splines and 20 B-spline functions are used in ξ and η directions, respectively, and the magnetic quantum numbers range from $m = -7$ to $m = 7$. The truncated range in the ξ direction is set as $\xi_{\max} = 2r_{\max}/R$ [23], where $r_{\max} = 150$ a.u. The time step is 0.1 a.u., and a $\cos^{1/8}$ absorber function is adopted near the boundary to avoid unphysical reflections of the electron wave packet from the boundary. Convergence is reached with the above settings.

In order to visualize internuclear distance and orientation effects, the ionization probability is normalized to its value of $\beta = 0^\circ$ unless otherwise indicated. Figure 1 depicts the ionization probability and the probabilities of electron spectra in different ranges obtained by TDSE for different R as a function of the angle β between the molecular axis and the laser polarization direction. Our calculation shows that the ionization yield is dominated by the ionized electron with energy less than 5ω. In Fig. 1(a), it is found that the ionization probability decreases monotonically with alignment angle β from 0° to 90° for $R = 2$ and 10 a.u., while an oscillatory behavior of the ionization probability with increasing alignment angle can be seen for $R = 20$ and 30 a.u. In the present work, the Keldysh parameter is $\gamma \approx 1$. For $R = 2$ a.u., the ratio $P_{\text{ion}}(90^\circ)/P_{\text{ion}}(0^\circ)$ is 0.585, which is close to the result of Ref. [24] ($\approx$0.5) for $\gamma = 0.92$ with $I = 3\times10^{14}$ W/cm^2. For $R = 10$ a.u., the ratio $P_{\text{ion}}(90^\circ)/P_{\text{ion}}(0^\circ)$ changes to 0.31, which indicates the ionization probability of $R = 10$ a.u. declines more quickly as a function of β with respect to that of $R = 2$ a.u., since charge-resonance-enhanced

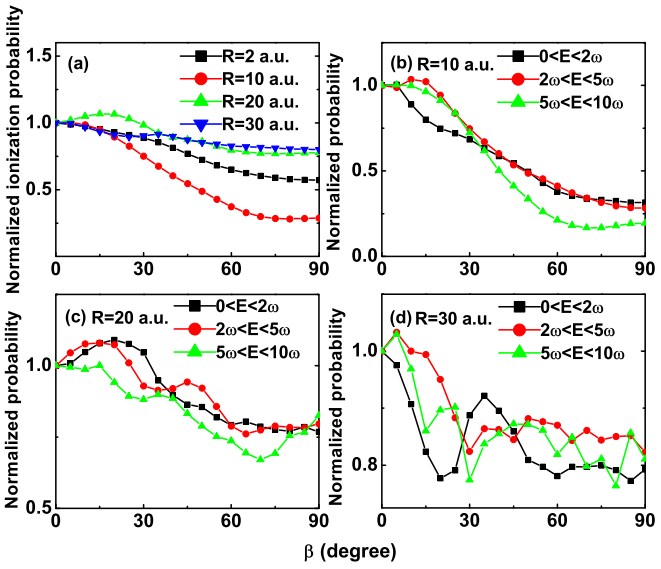

FIG. 1. (a) Normalized ionization probability as a function of alignment angle β with increasing internuclear separations obtained by TDSE (see text). (b)–(d) Normalized probabilities of electron spectra in different ranges versus β for $R = 10$, 20, and 30 a.u., respectively.

ionization occurs the most strongly at $R = 10$ a.u. with parallel alignment, becomes weak with increasing alignment angle β, and disappears for perpendicular alignment [25]. Molecular ions such as H_2^+ have pairs of electronic states known as charge-resonance states ($1\sigma_g$ and $1\sigma_u$ for H_2^+), which will be strongly coupled with external fields at large internuclear distance, giving rise to anomalously large ionization rates [16]. Accordingly, for $R = 10$ a.u., the probability of the electron in the continuum states shows a rapid decrease with increasing alignment angle β in Fig. 1(b), except for the probability in $[2\omega, 5\omega]$, which rises slightly before dropping quickly. For $R = 20$ a.u., the probabilities of electron spectra in the ranges $[0, 2\omega]$ and $[2\omega, 5\omega]$ first increase with β [see Fig. 1(c)], which accounts for the maximal ionization probability at $\beta = 15^\circ$ in Fig. 1(a). For $R = 30$ a.u., the oscillatory behavior of the probabilities in the ranges $[0, 2\omega]$ and $[2\omega, 5\omega]$ from $\beta = 0^\circ$ to $\beta = 60^\circ$ leads to the oscillation of the ionization probability in Fig. 1(a). The probabilities of $[0, 2\omega]$ and $[2\omega, 5\omega]$ change slowly between $\beta = 60^\circ$ and $\beta = 90^\circ$, which gives rise to the slight alteration of the ionization probability from $\beta = 60^\circ$ to $\beta = 90^\circ$ in Fig. 1(a). In general, the ionization probability of large-distance separations shows oscillation with respect to the alignment angle and the oscillation becomes faster for larger R. This can be attributed to the oscillation of the population of photoelectrons in low-energy continuum states. The oscillation becomes faster with increasing R and energy, which is a typical interference effect.

To gain more physical insight into the change of ionization dynamics for model diatomic molecules with increasing internuclear distances, two analytical model, i.e., Ammosov–Delone–Krainov (ADK) theory [26,27] and strong-field approximation (SFA) theory [28–30] are used to understand the above phenomena. In molecular ADK (MO-ADK) theory, the

alignment-dependent ionization rate reads

$$w(F,\mathbf{X}) = \sum_{m'} \frac{B^2(m')}{2^{|m'|}|m'|!} \frac{e^{-2\kappa^3/3F}}{\kappa^{2Z_c/\kappa-1}} \left(\frac{2\kappa^3}{F}\right)^{2Z_c/\kappa-|m'|-1}, \quad (2)$$

with

$$B(m') = \sum_l C_l D^l_{m',m}(\mathbf{X})(-1)^{m'} \sqrt{\frac{(2l+1)(l+|m'|)!}{2(l-|m'|)}}.$$

$D^l_{m',m}(\mathbf{X})$ is the rotation matrix and $\mathbf{X}$ is the Euler angle between the internuclear axis and the field direction. C_l is the asymptotic coefficient, F is the field strength, and $I_p = \kappa^2/2$ is the molecular ionization energy. When the internuclear distance is large, the model molecule is treated as two independent atomic systems, and each atomic system consists of one electron and one nucleus. The details of the tunneling ionization model for atoms can be found in Ref. [26], and the result in the present work is denoted "atomic ADK" theory (AADK).

In SFA theory, the ionization rate is calculated by length-gauge standard molecular SFA (SSFA) for $R = 2$ a.u. and modified dressed molecular SFA (DSFA) for large internuclear separations [28–30] due to the near degeneracy for the ground state and the first-excited state. For DSFA, the initial state is combined as an appropriate superposition of scaled hydrogen $1s$ atomic orbital as $\Phi(\mathbf{r},\mathbf{R}) = [\phi_{1s}(\mathbf{r}-\frac{\mathbf{R}}{2})e^{i\frac{\mathbf{R}}{2}\mathbf{A}(t)} + \phi_{1s}(\mathbf{r}+\frac{\mathbf{R}}{2})e^{-i\frac{\mathbf{R}}{2}\mathbf{A}(t)}]/\sqrt{2[1+S_{1s}(R)]}$, where $S_{1s}(R)$ indicates the atomic orbital overlap integral. The $1s$ orbital is expressed as $\phi_{1s}(\mathbf{r}) = \frac{1}{\sqrt{\pi}}\kappa^{3/2}e^{-\kappa\mathbf{r}}$, and $\kappa = \sqrt{2I_p}$. In S-matrix theory, the single ionization rate of a molecular ion exposed to the linearly polarized laser field with vector potential $\mathbf{A}(t) = E_0\mathbf{e}\cos\omega t$ is written as

$$W = 2\pi N_e \sum_{n=n_0}^{\infty} \int |T_{pn}|^2 \delta(E_p + I_p - n\omega) d\mathbf{P}, \quad (3)$$

and

$$T_{pn} = \frac{1}{T}\int_0^T dt \exp\left[i\left(\frac{E_0^2}{8\omega^3}\sin 2\omega t + \frac{E_0\mathbf{e}\cdot\mathbf{P}}{\omega^2}\sin\omega t\right)\right] \times \exp\left[i\left(\frac{P^2}{2} + I_p + U_p\right)t\right] E_0 \sin\omega t \widetilde{\phi}[\mathbf{P}+\mathbf{A}(t)], \quad (4)$$

with $\widetilde{\phi}(\mathbf{P}+\mathbf{A}(t)) = 2\cos(\mathbf{P}\cdot\mathbf{R}/2)d_{1s}(\mathbf{P}+\mathbf{A}(t))$, where $d_{1s}(\mathbf{P}+\mathbf{A}(t))$ indicates the atomic dipole moment of the $1s$ orbital. The trigonometric part $\cos(\mathbf{P}\cdot\mathbf{R}/2)$ shows dependence on the molecular structure and is related to the interference effect of the electron wave packets ionized from the two atomic centers. Although the vast majority of ionized electrons have small momenta, $\mathbf{P}\cdot\mathbf{R}$ is not negligible for large $\mathbf{R}$, and the trigonometric part $\cos(\mathbf{P}\cdot\mathbf{R}/2)$ plays an important role in molecular ionization for large internuclear distances. N_e indicates the number of equivalent electrons, and n_0 represents the minimum number of photons needed to ionize the electron. $E_p = P^2/2 + U_p$ denotes the quasienergy, where $P^2/2 = n\omega - U_p - I_p$ is the kinetic energy of the emitted electron after absorbing n photons, and U_p indicates the ponderomotive energy.

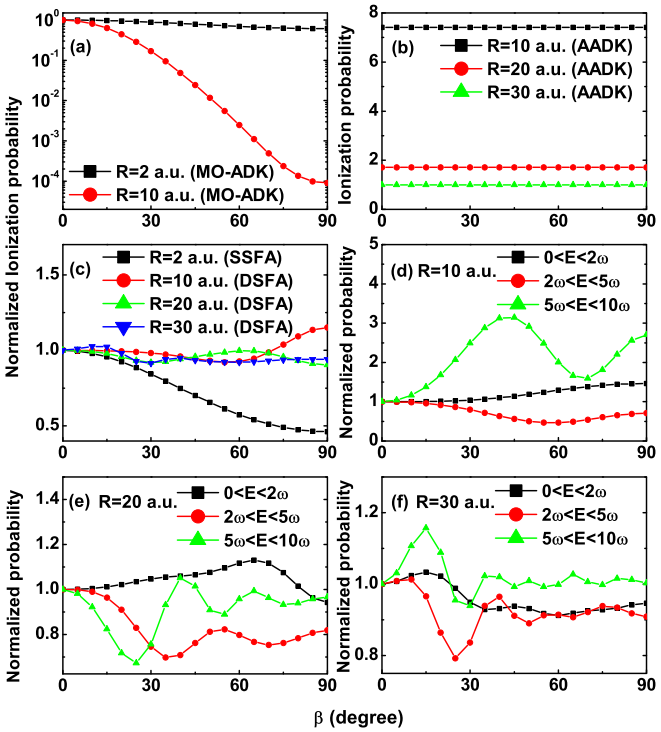

FIG. 2. (a), (b) Ionization probability versus β calculated from ADK theory. (c) Normalized ionization probability as a function of alignment angle β for different internuclear distances obtained by SFA (see text). (d)–(f) Normalized probabilities of electron spectra in different ranges calculated by DSFA with increasing β for $R = 10$, 20, and 30 a.u., respectively.

Figures 2(a) and 2(b) display the ionization probability calculated by ADK theory. For the results calculated by MO-ADK theory, the probability is normalized to its value at $\beta = 0°$. For $R = 2$ a.u., $P_{\rm ion}(90°)/P_{\rm ion}(0°)$ is 0.61, which is in a good agreement with the result of the TDSE (0.585). For $R = 10$ a.u., the probability obtained by MO-ADK decreases more quickly than that for $R = 2$ a.u. Although this behavior is qualitatively consistent with that of the TDSE result, the underlying mechanisms are completely different. In MO-ADK theory, the probability decreases fast due to the large nonspherical symmetry of the electronic density distribution, different from the TDSE calculation in which the decrease can be attributed to the charge-resonance effect. For the results obtained by AADK theory, the data do not show any dependence on the alignment angle β [Fig. 2(b)], which does not agree with the results of the TDSE calculation. In Fig. 2(b), we use the ionization rate of $R = 30$ a.u. as the unit, so the ionization probability increases with decreasing R because the nuclear charge and the ionization potential of the atomic system decrease with decreasing R in order to keep the ionization potential of the electron unchanged in the TDSE calculation.

Figures 2(c)–2(f) show the normalized ionization probability and normalized probabilities of electron spectra in different ranges as a function of the alignment angle calculated by SFA theory. Likewise, the ionization yield is mainly determined

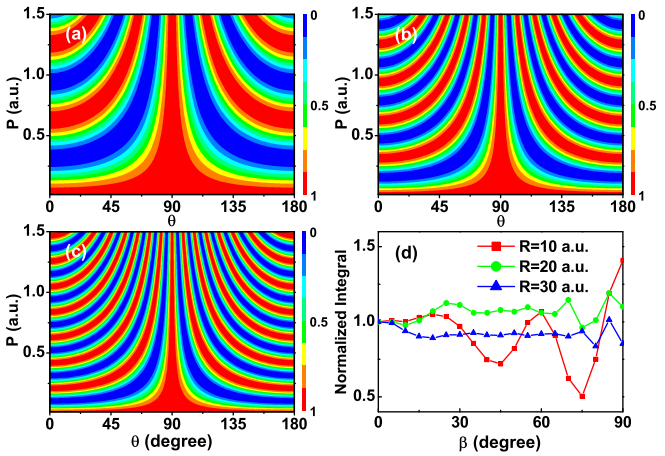

FIG. 3. (a)–(c) $\cos^2(\mathbf{P}\cdot\mathbf{R}/2)$ as a function of momentum of the emitted electron P and angle θ between $\mathbf{P}$ and the internuclear axis with increasing R. (d) Normalized integral versus alignment angle β with increasing R, obtained by the integral in a small solid angle (see text).

by the populations of electrons with energy less than 5ω. For $R = 2$ a.u., the ratio $P_{\rm ion}(90^\circ)/P_{\rm ion}(0^\circ)$ is 0.46, which also agrees well with that of TDSE (0.585). For large internuclear distances, the ionization probability oscillates with respect to alignment angle and the oscillation becomes faster when the internuclear distance increases, which is in qualitative agreement with the TDSE calculation. However, for $R = 10$ a.u., the ionization probability of $\beta = 90^\circ$ is larger compared with that of $\beta = 0^\circ$, which is inconsistent with the result of the TDSE calculation. This inconsistency can be attributed to the charge-resonance effect, which is responsible for the decrease of the ionization probability with alignment angle, as discussed above, which is not taken into account in the SFA calculation. Comparing Fig. 2(c) with Figs. 2(d)–2(f), one can find that, similar to the case of the TDSE calculation shown in Fig. 1, the oscillations in the ionization probability can be ascribed to the oscillations in the low-energy photoelectron spectra in which the frequency of the oscillation increases with increasing internuclear distance and photoelectron energy. Apparently, the interference effect originating from the factor $\cos^2(\mathbf{P}\cdot\mathbf{R}/2)$ in Eq. (4) gives rise to these oscillations which become faster with increasing R and P. In contrast, the ADK calculation shows no oscillation due to neglect of the interference effect [7].

To see the interference effect more clearly, we plot in Fig. 3 the distribution of $\cos^2(\mathbf{P}\cdot\mathbf{R}/2)$ as a function of momentum P of the ejected electron and the angle θ between $\mathbf{P}$ and the molecular axis with increasing R. In general, stripes appear periodically with the increase of P and θ. However, a closer inspection reveals some significant differences in the distribution of $\cos^2(\mathbf{P}\cdot\mathbf{R}/2)$ from Figs. 3(a) to 3(c). First, the frequency of the appearance of the stripes increases with increasing R for the same P and vice versa. Second, the width of the stripe becomes narrower with increasing internuclear distance R and momentum P. As we know, the electron is predominantly ejected along the laser polarization direction, so the ionization probability is mainly determined by the integral in a small solid angle around the laser polarization axis. Therefore, the main features of the SFA calculation in Fig. 2 can be well understood from Fig. 3. For example, at $\theta = 90^\circ$, the red stripe becomes narrower from $R = 10$ a.u. to $R = 30$ a.u., as shown in Figs. 3(a)–3(c). For $R = 10$ a.u., at alignment angle $\beta = 90^\circ$, the electron is primarily emitted along the direction at $\theta = 90^\circ$, and the factor $\cos^2(\mathbf{P}\cdot\mathbf{R}/2)$ has its maximum value along $\theta = 90^\circ$ for all momenta of emitted electrons (the red stripe around $\theta = 90^\circ$). However, at $\beta = 0^\circ$, the electron is mainly ejected along the direction at $\theta = 0^\circ$, and the value of $\cos^2(\mathbf{P}\cdot\mathbf{R}/2)$ shows alternative maximum and minimum with increasing P around $\theta = 0^\circ$. So the ionization yield at $\beta = 0^\circ$ is smaller compared with that at $\beta = 90^\circ$ for $R = 10$ a.u. For $R = 20$ a.u. and $R = 30$ a.u., the width of the red stripes near $\theta = 90^\circ$ become much narrower, thus the above phenomenon becomes less pronounced. Moreover, as the internuclear separation increases, the frequency of the oscillation for ionization probability increases and the oscillation amplitude decreases, which can both be attributed to the increasing frequency of the oscillation with increasing internuclear separation in Fig. 3. For comparison, we depict in Fig. 3(d) the normalized integrals calculated in a small solid angle (16°) along the laser direction for different R. The calculations qualitatively reproduce the main features in Fig. 2(c), including larger ionization probability of $\beta = 90^\circ$ than that of $\beta = 0^\circ$ for $R = 10$ a.u. and faster oscillation of the ionization probability with respect to β for larger R. In Ref. [31], the oscillatory behavior of the ionization yield for H_2^+ with R up to 6 a.u. in a high-frequency laser field is explained by a two-center interference effect arising from outgoing spherical waves.

III. CONCLUSION

In summary, we investigated the orientation-dependent ionization of model diatomic molecules with increasing internuclear separations up to 30 a.u. exposed to an intense few-cycle laser field based on the three-dimensional time-dependent Schrödinger equation. Our results show that the ionization probability decreases as a function of the angle between the laser field and the molecular axis for internuclear distances $R = 2$ and 10 a.u., wherein the ionization yields show oscillation with increasing alignment angles for large internuclear separations of $R = 20$ and 30 a.u. Compared with the calculations based on ADK theory and S-matrix theory, the interesting oscillatory behavior of ionization probability for large internuclear distances is ascribed to the interference of low-energy electron wave packets ionized from the two cores. Moreover, it is found that ADK theory is only valid for molecules with small internuclear distance but fails for large R due to neglect of the interference effect. Our work provides a further understanding of strong-field phenomena such as molecular orientation ionization and molecular dissociative ionization.

ACKNOWLEDGMENTS

This work was partially supported by the National Basic Research Program of China (Grant No. 2013CB922201) and the NNSF of China (Grants No. 11274050, No. 11334009, No. 11425414, No. 11374197, No. 11447114, and No. 11504215).

[1] J. Itatani *et al.*, Nature (London) **432**, 867 (2004).
[2] C. Blaga *et al.*, Nature (London) **483**, 194 (2012).
[3] J. H. Posthumus, Rep. Prog. Phys. **67**, 623 (2004).
[4] A. Talebpour, C.-Y. Chien, and S. L. Chen, J. Phys. B: At., Mol. Opt. Phys. **29**, L677 (1996).
[5] C. Guo. M. Li, J. P. Nibarger, and G. N. Gibson, Phys. Rev. A **58**, R4271(R) (1998).
[6] J. Muth-Böhm, A. Becker, and F. H. M. Faisal, Phys. Rev. Lett. **85**, 2280 (2000).
[7] Z. Y. Lin *et al.*, Phys. Rev. Lett. **108**, 223001 (2012).
[8] D. Pavičić, K. F. Lee, D. M. Rayner, P. B. Corkum, and D. M. Villeneuve, Phys. Rev. Lett. **98**, 243001 (2007).
[9] D. A. Telnov and Shih-I Chu, Phys. Rev. A **79**, 041401(R) (2009).
[10] M. Abu-samha and L. B. Madsen, Phys. Rev. A **80**, 023401 (2009).
[11] S. Petretti, Y. V. Vanne, A. Saenz, A. Castro, and P. Decleva, Phys. Rev. Lett. **104**, 223001 (2010).
[12] V. P. Majety and A. Scrinzi, Phys. Rev. Lett. **115**, 103002 (2015).
[13] L. B. Madsen, L. A. A. Nikolopoulos, T. K. Kjeldsen, and J. Fernández, Phys. Rev. A **76**, 063407 (2007).
[14] M. Awasthi, Y. V. Vanne, A. Saenz, A. Castro, and P. Decleva, Phys. Rev. A **77**, 063403 (2008).
[15] A. S. Simonsen, S. A. Sørngård, R. Nepstad, and M. Førre, Phys. Rev. A **85**, 063404 (2012).
[16] T. Zuo and A. D. Bandrauk, Phys. Rev. A **52**, R2511 (1995).
[17] A. Saenz, Phys. Rev. A **61**, 051402 (2000).
[18] E. Constant, H. Stapelfeldt, and P. B. Corkum, Phys. Rev. Lett. **76**, 4140 (1996).
[19] Z. Ansari *et al.*, New J. Phys. **10**, 093027 (2008).
[20] J. Henkel, M. Lein, and V. Engel, Phys. Rev. A **83**, 051401(R) (2011).
[21] H. Bachau, E. Cormier, P. Decleva, J. E. Hansen, and F. Martín, Rep. Prog. Phys. **64**, 1815 (2001).
[22] S. L. Hu, Z. X. Zhao, and T. Y. Shi, Int. J. Quantum Chem. **114**, 441 (2014).
[23] B. Zhang, J. M. Yuan, and Z. X. Zhao, Phys. Rev. A **85**, 033421 (2012).
[24] G. L. Kamta and A. D. Bandrauk, Phys. Rev. A **71**, 053407 (2005).
[25] T. K. Kjeldsen, L. B. Madsen, and J. P. Hansen, Phys. Rev. A **74**, 035402 (2006).
[26] M. V. Ammosov, N. B. Delone, and V. P. Krainov, Zh. Eksp. Teor. Fiz. **91**, 2008 (1986) [Sov. Phys. JETP **64**, 1191 (1986)].
[27] X. M. Tong, Z. X. Zhao, and C. D. Lin, Phys. Rev. A **66**, 033402 (2002).
[28] D. B. Milošević, Phys. Rev. A **74**, 063404 (2006).
[29] J. Chen and S. G. Chen, Phys. Rev. A **75**, 041402(R) (2007).
[30] W. Becker, J. Chen, S. G. Chen, and D. B. Milošević, Phys. Rev. A **76**, 033403 (2007).
[31] S. Selstø, M. Førre, J. P. Hansen, and L. B. Madsen, Phys. Rev. Lett. **95**, 093002 (2005).